UNIVERSIDADE ESTADUAL PAULISTA
"JÚLIO DE MESQUITA FILHO"
Campus de São José dos Campos
Instituto de Ciência e Tecnologia

MATHEUS TAE GEUN GONÇALVES JANG

Increased chlorophyll-*a* concentration in Barra Bonita reservoir during extreme drought periods

São José dos Campos

2022

Matheus Tae Geun Gonçalves Jang

Increased chlorophyll-*a* concentration in Barra Bonita reservoir during extreme drought periods

Trabalho de graduação apresentado como requisito parcial para a obtenção do título de Bacharel em Engenharia Ambiental pela Universidade Estadual Paulista "Júlio de Mesquita Filho".

Orientador: Prof. Assoc. Enner Alcântara

São José dos Campos

2022

Instituto de Ciência e Tecnologia [internet]. Normalização de tese e dissertação [acesso em 2023]. Disponível em http://www.ict.unesp.br/biblioteca/normalizacao

Apresentação gráfica e normalização de acordo com as normas estabelecidas pelo Serviço de Normalização de Documentos da Seção Técnica de Referência e Atendimento ao Usuário e Documentação (STRAUD).

Jang, Matheus Tae Geun Gonçalves
Increased chlorophyll-a concentration in Barra Bonita reservoir during extreme drought periods
/ Matheus Tae Geun Gonçalves Jang. - São José dos Campos : [s.n.], 2022.
45 f. : il.

Trabalho de Conclusão de Curso (TCC) - Graduação em Engenharia Ambiental - Universidade Estadual Paulista (Unesp), Instituto de Ciência e Tecnologia, São José dos Campos, 2022.
Orientador: Enner Alcântara.

1. Eventos extremos. 2. Sensoriamento remoto. 3. Floração de algas. 4. Corpos hídricos continentais. I. Alcântara, Enner, orient. II. Universidade Estadual Paulista (Unesp), Instituto de Ciência e Tecnologia, São José dos Campos. III. Universidade Estadual Paulista TJúlio de Mesquita FilhoT - Unesp. IV. Universidade Estadual Paulista (Unesp). V. Título.

Ficha catalográfica elaborada pela Biblioteca Prof. Achille Bassi e Seção Técnica de Informática, ICMC/USP com adaptações - STATI, STRAUD e DTI do ICT/UNESP.
Renata Aparecida Couto Martins CRB-8/8376

Matheus Tae Geun Gonçalves Jang

Increased chlorophyll-a concentration in Barra Bonita reservoir during extreme drought periods

Trabalho de graduação apresentado como requisito parcial para a obtenção do título de Bacharel em Engenharia Ambiental pela Universidade Estadual Paulista "Júlio de Mesquita Filho".

São José dos Campos, 16 de dezembro de 2022.

BANCA EXAMINADORA

Prof. Assoc. Enner Alcântara

ICT/Unesp

Prof. Assoc. Fernando Luiz Campos Carvalho

ICT/Unesp

Dra. Luciana de Resende Londe

Cemaden

DEDICATÓRIA

Dedico esse trabalho a pessoas extremamente especiais, pessoas que participaram de todo esse processo comigo, que me viram chorando e comemorando. Obrigado, pai e mãe. Vocês são os meus verdadeiros “sem vocês, isso não aconteceria”. Depois de tantos altos e baixos, de tantos empecilhos e também de tanta felicidade, nós conseguimos.

Não poderia deixar de dedicar tudo isso aos meus tios, Cleber e Hellen, e às minhas irmãs, Bia e Isa. Tio, tia, obrigado por serem meus segundos pais. Obrigado por terem me possibilitado tanto, por nunca terem me deixado desistir. Meninas, assim como falo para o papai e para mamãe, essa é a nossa conquista. Obrigado por compartilharem isso comigo, vocês são minha força.

AGRADECIMENTOS

Agradeço, antes de tudo, a Deus. Sem tua companhia, que sempre me trouxe paz, esperança e força, eu jamais teria conseguido chegar onde cheguei. Jamais chegarei onde quero chegar.

Agradeço imensamente aos meus pais, que sempre me incentivaram e tornaram possível a realização desse sonho. Sem vocês, eu não teria as forças necessárias para passar pelas grandes dificuldades, nem felicidade em compartilhar as grandes conquistas. Aproveito para agradecer, com todo coração, a minha família, que me sempre me deu todo o suporte que eu poderia precisar.

Não poderia deixar de agradecer meus amigos. Conheci pessoas incríveis durante a graduação, que estiveram do meu lado nos piores e nos melhores momentos, vocês tornaram tudo mais fácil e prazeroso. Um agradecimento especial para vocês, Lucas e Bari. Vocês foram meus companheiros de sala e de casa por todo esse tempo, sou imensamente grato por ter compartilhado tanto com vocês. Obrigado aos meus grandes amigos de infância (Grand, Breno, Danilo, Fal, Artur e Jão) que, mesmo muitas vezes longe, sempre estiveram tão próximos. Obrigado Thais, por ter me acompanhado, também de longe, mas sempre com tanto carinho e cuidado nessa jornada.

Um agradecimento mais que especial para meu orientador, Enner Alcântara. Obrigado por, antes de tudo, acreditar em mim e no meu potencial. Trabalhamos juntos por um bom tempo e, mesmo passando por obstáculos, você jamais deixou de me apoiar e incentivar. Obrigado também a todos os professores do DEA que compartilharam seus conhecimentos comigo. Hoje tenho certeza de que vocês, professores, são um dos grandes responsáveis pela formação de seres humanos cada vez melhores!

Por fim, um agradecimento gigantesco ao CNPq por não apenas uma, mas duas bolsas PIBIC durante a execução desse longo projeto. Ambas foram de extrema importância para que eu fosse capaz de finalizar o trabalho. Obrigado pelo apoio à pesquisa. Que essa prática jamais se perca e que os incentivos aumentem cada vez mais. A pesquisa científica tem um poder imenso na sociedade e jamais deve ser ignorada!

RESUMO

Modelos de projeção climática indicam que são esperados longos períodos de seca dentro dos próximos 100 anos em várias partes da América do Sul. Para entender os efeitos dos longos períodos de seca em ambientes aquáticos, nós investigamos a resposta da concentração da clorofila-*a* (Chl-*a*) a recentes eventos de seca extrema no Reservatório da Hidrelétrica de Barra Bonita (RHBB) no estado de São Paulo, Brasil. Nós usamos imagens de satélite para estimar a concentração de Chl-*a* de 2014 a 2020 usando o Índice Slope (NRMSE de 18,92% e bias de -0.20 mg m^{-3}). Dados auxiliares de precipitação, nível d'água e temperatura do ar para o mesmo período também foram usados. Eventos de seca foram identificados usando o índice de precipitação padronizada (SPI). Em complemento, nós computamos a probabilidade de futuros eventos de seca. Dois períodos mostraram condições de seca extrema: 1) janeiro – fevereiro (2014) e 2) abril – maio (2020). Ambos os períodos foram caracterizados como probabilidade de recorrência de 1 a cada 50 anos. A maior correlação foi observada entre concentração de Chl-*a* e SPI (-0.97) em 2014, enquanto Chl-*a* teve maior correlação com nível d'água (-0.59) em 2020. Esses resultados fornecem novos conhecimentos acerca da influência de eventos de seca extrema sob a concentração de Chl-*a* no RHBB e sua relação com outras variáveis climáticas e níveis d´água dos reservatórios. Eventos de seca implicam em menos chuvas, temperaturas mais altas e secas atmosféricas, e esses fatores afetam evaporação e o nível d'água dos reservatórios.

Palavras-chave: eventos extremos; sensoriamento remoto; floração de algas; corpos hídricos continentais.

ABSTRACT

Climate projections models indicate that longer periods of droughts are expected within the next 100 years in various parts of South America. To understand the effects of longer periods of droughts on aquatic environments, we investigated the response of chlorophyll-a (Chl-*a*) concentration to recent severe drought events in the Barra Bonita Hydroelectric Reservoir (BBHR) in São Paulo State, Brazil. We used satellite imagery to estimate the Chl-*a* concentration from 2014 to 2020 using the Slope Index (NRMSE of 18.92% and bias of -0.20 mg m^{-3}). Ancillary data such as precipitation, water level and air temperature from the same period were also used. Drought events were identified using the standardized precipitation index (SPI). In addition, we computed the probability of future drought events. Two periods showed extremely dry conditions: 1) January - February (2014) and 2) April - May (2020). Both periods were characterized by a recurrence probability of 1 in every 50 years. The highest correlation was observed between Chl-*a* concentration and SPI (-0.97) in 2014, while Chl-*a* had the highest correlation with water level (-0.59) in 2020. These results provide new insights into the influence of extreme drought events on the Chl-*a* concentration in the BBHR and their relationship with other climate variables and reservoir water levels. Drought events imply less rainfall, higher temperatures, and atmospheric dryness, and these factors affect evaporation and the water levels in the reservoir.

Keywords: extreme events; remote sensing; algae bloom; inland waters body.

SUMÁRIO

1 INTRODUÇÃO

Condições climáticas, tais como, precipitação, vento e passagem de frentes frias, exercem papel importante sobre o padrão de mistura e estratificação da coluna d`água de sistemas aquáticos (CURTARELLI et al., 2014), consequentemente, o clima de luz na coluna d`água (TUNDISI et al., 2010). A mistura da coluna d`água e o tempo de residência da água no sistema aquático são apontados como os responsáveis mais importantes para a riqueza de espécies de fitoplâncton em reservatórios (MATSUMURA-TUNDISI, TUNDISI, 2005). Por outro lado, a predominância para determinadas espécies é frequentemente associada com a estratificação termal e a estabilidade da coluna d`água (TUNDISI et al., 2010). Portanto, florações de cianobactérias ocorrem no outono, quando o tempo de residência da água é maior, enquanto, chlorophytas e diatomáceas são mais comuns durante a primavera e o verão, quando o tempo de residência é menor (PERRY et al., 1990).

A região sudeste do Brasil passou por um longo período de seca, que começou em 2012 e se estendeu até 2015. De acordo com Getirana (2016) uma perda de água de aproximadamente 6.1 cm/ano foi observada durante o período de seca mencionado. A baixa precipitação levou a redução do volume útil de sistemas aquáticos e, consequentemente, uma crise de abastecimento público. Em reservatórios, a baixa precipitação afeta o tempo de residência da água e a cota, devido ao controle de fluxo.

Em ambientes aquáticos produtivos, o estado trófico continua a aumentar, quando a precipitação é reduzida e o tempo de residência aumenta.

Watanabe et al. (2016) realizaram um experimento de curto termo no reservatório de Barra Bonita, com o objetivo de verificar se a seca de 2014 teve impacto na concentração de clorofila-*a*. Os autores concluíram que a seca de 2014 contribuiu para um aumento da floração de algas no reservatório. O estudo de Watanabe e colaboradores não levou em consideração a fenologia do fitoplâncton no reservatório, portanto, não compararam anos anteriores, com o evento de seca de 2014.

2 ARTIGOS SUBMETIDOS E/OU APROVADOS

2.1 Artigo – Matheus Tae Geun Jang[a], Enner Alcântara[a],*, Thanan Rodrigues[b], Edward Park[c], Igor Ogashawara[d], José A. Marengo[e]

Increased chlorophyll-*a* concentration in Barra Bonita reservoir during extreme drought periods

[a] Institute of Science and Technology, São Paulo State University, São José dos Campos, São Paulo, Brazil.

[b] Federal Institute of Education, Science and Technology of Brasília, DF, Brazil.

[c] National Institute of Education and Earth Observatory of Singapore, Nanyang Technological University, Singapore.

[d] Leibniz-Institute of Freshwater Ecology and Inland Fisheries, 16775, Stechlin, OT, Neuglobsow, Germany.

[e] National Center for Monitoring and Early Warning of Natural Disasters (Cemaden), São José dos Campos, Brazil

---

‡ Artigo elaborado de acordo com as normas do Periódico *Science of The Total Environment* (*Print version* ISSN 0048-9697). Publicado em: 04/07/2022.
* Corresponding author: enner.alcantara@unesp.br

Abstract

Climate projections models indicate that longer periods of droughts are expected within the next 100 years in various parts of South America. To understand the effects of longer periods of droughts on aquatic environments, we investigated the response of chlorophyll-a (Chl-a) concentration to recent severe drought events in the Barra Bonita Hydroelectric Reservoir (BBHR) in São Paulo State, Brazil. We used satellite imagery to estimate the Chl-a concentration from 2014 to 2020 using the Slope Index (NRMSE of 18.92% and bias of -0.20 mg m-3). Ancillary data such as precipitation, water level and air temperature from the same period were also used. Drought events were identified using the standardized precipitation index (SPI). In addition, we computed the probability of future drought events. Two periods showed extremely dry conditions: 1) January - February (2014) and 2) April - May (2020). Both periods were characterized by a recurrence probability of 1 in every 50 years. The highest correlation was observed between Chl-a concentration and SPI (-0.97) in 2014, while Chl-a had had the highest correlation with water level (-0.59) in 2020. These results provide new insights into the influence of extreme drought events on the Chl-a concentration in the BBHR and their relationship with other climate variables and reservoir water levels. Drought events imply less rainfall, higher temperatures, and atmospheric dryness, and these factors affect evaporation and the water levels in the reservoir.

Keywords: Extreme events, remote sensing, algae bloom, inland waters body.

1. Introduction

Phytoplankton are essential for the functioning of aquatic systems. In particular seasonal blooms are major sources of energy for higher trophic levels organisms (Smayda, 1997). When phytoplankton naturally accumulate faster than it dies, phytoplankton blooms occur. However, when phytoplankton growth is affected by anthropogenic inputs of nutrients aquatic environments become degraded (Paerl et al., 2014). Phytoplankton biomass can be identified through a proxy, the chlorophyll-a (Chl-*a*) concentration, which is commonly monitored by water quality programs. Notably, phytoplankton blooms have been reported regularly in lakes, reservoirs, coastal areas, and oceans worldwide (Behrenfeld et al., 2014).

Temporal and seasonal variations in phytoplankton is known as phenology, which responds much more quickly to meteorological and climatic forces than to terrestrial vegetation (Palmer et al., 2015). Phenological responses to environmental changes include: 1) shifts in the timing of phytoplankton blooms (Berger et al., 2010), 2) changes in phytoplankton biomass (Elliot et al., 2006), 3) changes in their growth rates (Maberly et al., 1994), and 4) changes in overall biodiversity (Elliot, 2012). Understanding phytoplankton phenology can help to identify the environmental drivers in aquatic systems change, especially when phytoplankton blooms are associated with nutrients budgets, land use and land cover, and climatic variables (Gittings et al., 2018). While the traditional monitoring of phytoplankton biomass is labor-and-cost intensive, satellite data have been used to as an alternative to estimate and monitor Chl-*a* concentrations in inland waters (Moses et al., 2009, Matthews 2011, Mishra and Mishra, 2012).

Monitoring aquatic systems is important because climatic extremes such as drought, is severely threatening aquatic ecosystems globally (Rosenzweig et al. 2007). However, understanding the potential effects of climate variability on aquatic systems is challenging because of the multitude of responses in the entire watershed. The chemical, biological, and physical responses of aquatic systems are affected by climate extremes (Rosenzweing et al., 2007, Williamson et al., 2008, Adrian et al., 2009). Drought have recently increased in frequency, intensity, and duration resulting in the occurrence of intense and long dry periods (Cunha et al., 2019). In Brazil, drought periods have become increasingly frequent, resulting in episodes of water deficit leading to water crises in southeastern Brazil (Nobre et al., 2016, Getirana et al., 2021). In addition, water deficits mean there is a higher risk of fires and there was a record number of fires in Amazonia and Pantanal (Marengo et al 2021, Correa et al., 2022). Getirana (2016) estimated terrestrial water storage anomalies for the drought in southeastern Brazil from 2012 to 2015 and established that the drought started when a water loss rate of -6.1 cm/year was detected in the region. Extreme drought is mostly related to lower-than-usual precipitation rates, resulting in high soil moisture depletion and lower rates of evapotranspiration. A reduction of 20–23% in precipitation over an extended period of three years is sufficient to induce serious water scarcity in the country. During this period, low precipitation rates led to a reduction in the levels of the Cantareira System reservoir. January 2014 was the driest in several decades, and with record high temperatures, it contributed to one of the worst water crisis in history (Nobre et al., 2016).

Intensification (in space and time) of algal growth in inland waters has been linked to eutrophication and climate variability; however, there is little empirical evidence that this trend is universal (Wilkinson et al., 2022). Ho et al. (2019) used three decades of Landsat-5/Thematic Mapper (TM) imagery to investigate long-term trends in intense summertime near-surface phytoplankton blooms in 71 large lakes worldwide. This study found that the summertime bloom intensity increased in 68% of the studied lakes. In contrast, Hallegraeff et al. (2021) analyzed a global dataset extracted from the Harmful Algal Event Database and Ocean Biodiversity Information System for the period 1985–2018 and found no uniform global trend for harmful marine algae. These studies suggest that future research should focus on regional rather than global trends. One recent study used 2.91 million Landsat images from 1982 to 2019 to characterize algal blooms in 248,243 lakes worldwide and showed that the occurrence of algal blooms has increased in the last four decades (Hou et al., 2022). Although the relationship between phytoplankton growth and climate variability remains controversial, many studies have used remote sensing techniques to investigate their occurrence and intensity (Ho et al., 2019, Hou et al., 2022).

In Brazil, Watanabe et al. (2016) studied the effect of the 2014 drought on the Chl-*a* concentration in Barra Bonita Hydroelectric Reservoir (BBHR). In this study, field data from May to October showed an increase in the Chl-*a* concentration during the most severe period of drought. However, this study did not cover the temporal dynamics of the Chl-*a* concentrations during the 2014 drought. The lack of time-series analysis limits the understanding of the relationship between the observed increase in Chl-*a* in the BBHR and drought events. To address this knowledge gap, this current study evaluated the relationship between the Chl-*a* concentration and precipitation, air temperature, water level, and drought time series (from 2014 to 2020). Our goal was to understand phytoplankton responses to drought events in eutrophic subtropical aquatic systems.

2. Materials and methods

2.1 Study area

BBHR is a storage-type system (flooded area of 310 km^2, volume of 3.62×106 m^3), and is in the middle course of the Tietê River, São Paulo State, Brazil (Figure 1). The average depth of water is 25 m with a retention time ranging from 37 to 137 days (Barbosa et al., 1999). The hydroelectric dam has been operational since 1963 and the dam has multiple uses, including power generation, fishing, recreation, and navigation. The BBHR is a eutrophic aquatic environment, and it is also classified as meso-to-hypertrophic (Smith et al., 2014; Watanabe et al., 2015) as it receives a high load of pollutants from large urban centers in the São Paulo and Piracicaba regions (Smith et al., 2014). Additionally, nonpoint source pollution has been reported to be responsible for eutrophication in aquatic systems (Tundisi et al., 2008). Because of its high trophic level, BBHR is an emitter of greenhouse gases, such as methane (CH4), carbon dioxide (CO2), and nitrous oxide (NO2) (Abe et al., 2003).

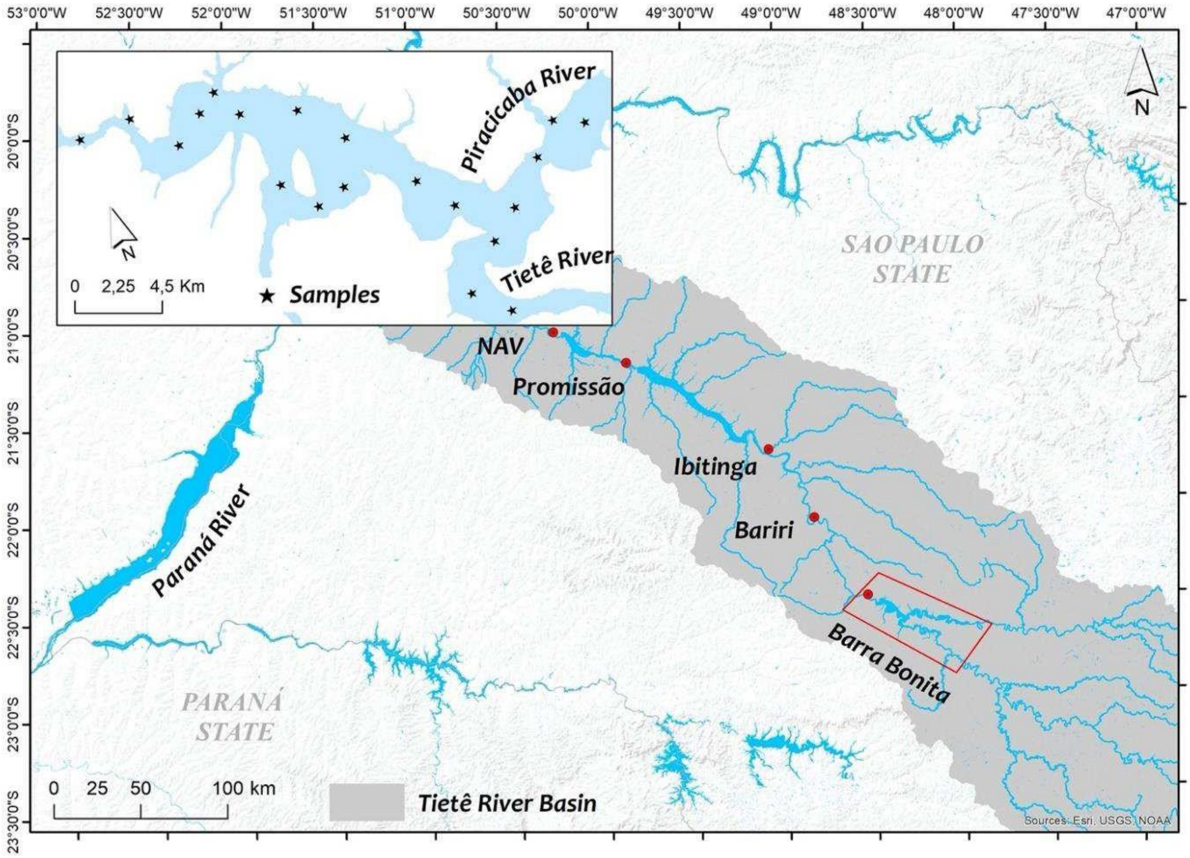

Figure 1. Location of Barra Bonita Hydroelectric Reservoir (BBHR) in São Paulo State, Brazil and sampling distribution.

2.2. Field survey

Proximal sensing data and Chl-*a* concentrations were measured during two field campaigns conducted in BBHR from (1) 4–9 May 2014, during austral autumn or the end of the rainy period, and (2) 13–16 October 2014, during austral spring or the end of the dry season. Forty samples (20 in each field survey) were collected from the subsurface (0.5 m). After reviewing the collected data, five samples were identified as outliers (based on Cook's distance method) and excluded from the analysis. More information about the data collection protocols and data processing can be found in Bernardo et al. (2018). In addition, the statistical tests used for water quality analysis can be found in Watanabe et al. (2018).

Proximal sensing data (hyperspectral radiance and irradiance) were collected using TriOS/RAMSES (ACC-VIS and ARC-VIS) optical sensors (http://www.trios.de). These sensors were developed by the TriOS company in Germany with 190 channels between 320 and 950 nm, a spectral resolution of 3.3 nm and an accuracy of 0.3 nm. The viewing geometry of the radiometric data acquisition was based on the method by Mobley (1999), and the remote sensing reflectance (R_{rs}, sr^{-1}) was calculated with Equation 1:

$$R_{rs}(\theta,\varphi,\lambda) = \frac{L_t(\theta,\varphi,\lambda) - \rho \times L_{sky}(\theta,\varphi,\lambda)}{E_d(\lambda)} \quad (1)$$

where L_t is the total radiance, which represents the sum of the water-leaving radiance (L_w) and the surface-reflected radiance (L_r); L_{sky} is the sky radiance; ρ is defined as the ratio between L_r and L_{sky} in one direction; and E_d is the incident irradiance on the water surface. R_{rs} was calculated with a method proposed by Lee et al. (2010) whereby the spectral ρ variation was considered.

In situ R_{rs} data were resampled to represent the Landsat-8/Operational Land Imager (OLI) spectral bands based on the relative spectral response function of each spectral band (Barsi et al., 2014) (Equation 2).

$$R_{rs}^{OLI} = \frac{\int_{\lambda_{min}}^{\lambda_{max}} R_{rs}(\lambda) \times S_{RF}(\lambda)}{\int_{\lambda_{min}}^{\lambda_{max}} S_{RF}(\lambda)} \quad (2)$$

where R_{rs}^{OLI} is the convoluted in situ R_{rs} for the OLI bands; S_{RF} is the spectral response function for each band, and λ_{max} and λ_{min} are the longer and shorter wavelengths in each band respectively.

The Chl-*a* concentration was determined after filtering the subsurface water samples with 0.7 µm Whatman GF/F filters (GE Healthcare, Chicago, IL, USA. Chl-*a* was extracted using 90% acetone solution, as proposed by Golterman et al. (1978).

2.3. Precipitation and water level data

Precipitation data were calculated from the high-resolution multi-satellite precipitation product (Integrated Multi-satellite Retrievals for Global Precipitation Measurement – GPM-IMERG) that have a spatial resolution of 0.1° and a temporal resolution of one day (Huffman et al., 2019). Water level data were obtained from the online database Hidroweb of the Brazilian National Water Agency (https://www.gov.br/ana/pt-br).

2.4. Drought assessment and return period

Drought periods were identified using the Standardized Precipitation Index (SPI, McKee et al., 1993). The SPI analyzes dry and wet periods based on the probability of precipitation, and it was developed to quantify the precipitation deficit in a specified period. The minimum input period for this analysis corresponds to 3 months.

The return period (RP) is the inverse of the probability (P) of an event. The probability of an event was calculated empirically for each drought class using the quotient of the total number of events (N) in the study period and the length of the study period in days (n) as PR = 1/P = N/n (Ridder et al., 2020).

2.5. Satellite images

The Landsat-8 Surface Reflectance Product that covers the area of BBHR was acquired from the USGS Earth Explorer database (https://earthexplorer.usgs.gov) for the period between 2014 and 2020. A total of 50 cloud-free images were obtained. The use of the Surface Reflectance Product was previously validated for this study site and this product was found to perform better than other atmospheric correction methods (Bernardo et al., 2017). The Surface Reflectance Product was atmospherically corrected and generated using the Landsat-8 Surface Reflectance Code (LASRC), which yields surface reflectance at a 30-m spatial resolution, which is suitable for studying the dynamics of our study site (Silva et al., 2021). Surface reflectance was then converted into R_{rs} by dividing it by π.

2.6. Chl-a estimation and trophic state classification

To estimate the Chl-*a* concentration from satellite imagery, we used the slope index proposed by Mishra and Mishra (2010, Equation 3) and empirically calibrated it with our field dataset (Equation 4). The slope index was selected because of its high performance in the estimation of the Chl-*a* concentration using MSI/Sentinel 2A imagery for the BBHR (Watanabe et al., 2019). In situ R_{rs} data were resampled to represent the OLI/Landsat-8 bands using the relative spectral response function of each OLI spectral band (Barsi et al., 2014).

$$Slope = \frac{R_{\mathrm{rs}}(\lambda_2) - R_{\mathrm{rs}}(\lambda_1)}{\lambda_2 - \lambda_1} \quad (3)$$

$$Chl - a = -4.106 \times Slope - 28.862 \quad (4)$$

where λ_1 is the green spectral band and λ_2 is the red spectral band of OLI/Landsat-8. Chl-*a* is given in mg.m^{-3}.

The validation was calculated using leave-one-out cross-validation (LOOCV, Arlot and Celisse, 2010). An accuracy assessment was performed using the normalized root mean square error (NRMSE) and bias (Equations 5 and 6).

$$NRMSE = \frac{RMSE}{y_{max} - y_{min}} \times 100 \quad (5)$$

$$Bias = \frac{\sum_{i=1}^{n} (y_i^E - y_i^M)}{n} \quad (6)$$

where y_i^E is the estimated value for i observation, y_i^M is the measured value for i observation, y_{max} is the maximum measured value, y_{min} is the minimum measured value, and $y_{average}^M$ is the average measured value.

The Chl-*a* concentration dataset estimated from the OLI/Landsat-8 images was used to calculate the trophic state index (TSI). This index classifies aquatic systems into different trophic levels, allowing water quality evaluation. In this study, TSI was calculated based on the equations proposed by Carlson (1977) and modified by Toledo et al. (1983) and this method only use the Chl-*a* concentration for the calculation of TSI (Equation 7). The limits for different TSI classes are listed in Table 1.

$$TSI = 10 \times (6 - \frac{2.04 - 0.68 lnChl-a}{ln2}) \quad (7)$$

Table 1. Limits for different TSI classes according to the Carlson (1977) classification after the modifications by Toledo et al. (1990).

TSI	Criterion
Ultraoligotrophic	≤ 24
Oligotrophic	24 < TSI ≤ 44
Mesotrophic	44 < TSI ≤ 54
Eutrophic	54 < TSI ≤ 74
Hypereutrophic	TSI > 74

2.7. Chl-a time series analysis

Water quality data often do not follow well defined probability distributions, such as normal and lognormal (Lettenmaier et al., 1991). Hence, probability plots were used to determine how well the data fit the theoretical distribution. The first step in analyzing the Chl-*a* dataset was to find the best distribution fitting, and we tested the following distributions: exponential, Fisher–Tippett, Gamma, Gumbel, log-normal, logistic, normal, student, and Weibull. To select the best-fit distribution, we used the Kolmogorov–Smirnov test (K-S), which is a nonparametric test based on the maximum absolute deviation (D) between the two functions of the cumulative distribution (Equation 8).

$$D = \max f_n(x) - F_0(x) \quad (8)$$

where $F_n(x)$ is the cumulative density function based on n measurements and $F_0(x)$ is the specified theoretical cumulative distribution function under the null hypothesis H_0. The values of D (n, α) are provided in the tables (Hann, 1977). If $D \geq D(n, \alpha)$, the H_0 hypothesis is rejected, and if $D < D(n, \alpha)$, H_0 is accepted for the chosen level of significance $\alpha = 0.05$.

Chl-*a* time series were analyzed for autocorrelation using Durbin–Watson (DW) and for seasonality using Augmented Dickey–Fuller (ADF) tests. The DW test is widely used for autocorrelation in non-lagged dependent variables and when sample sizes are smaller. It ranges from 0 to 4, and when values are close to 2, there is no autocorrelation; when values are close to 0, there is a positive autocorrelation; and when values are close to 4, there is a negative autocorrelation (Durbin and Watson, 1950, 1951). The ADF stationarity test was used to check for stability of the mean, standard deviation, and presence of seasonality (Fuller, 1996). The null hypothesis is that the time series possesses a unit root and is non-stationary. If seasonality is present in the time series, the data are not stationary.

Trend analysis was performed using the Mann–Kendall test (Yue and Wang, 2004) which considers the null hypothesis as having no trend. Additionally, the Theil–Sen Robust Linear Regression (TS) test was used to confirm the time series trends (Sen, 1968). The Theil–Sen test is a median-based and nonparametric test that does not make assumptions about the dataset distribution and outliers have on effect on the results.

3. Results

3.1. Drought assessment

Drought occurred during two periods of extreme dryness, in: 1) January and February of 2014, and 2) April and May of 2020 (Figure 2). In addition, severe dry conditions were observed for the following periods: 1) July and November of 2014; 2) March of 2017; 3) February and May of 2018, and 4) January of 2019. Notably, the two extreme dry periods occurred during Austral summer in 2014 and the austral autumn in 2020.

For the months of January and February of 2014 the values for SPI, rainfall, air temperature and water level were -2.36 and -2.74, 104 mm and 112 mm, 26.1 ℃ and 26.8 ℃, 449 m (utilizable storage capacity of 78.74%) and 449.44 (utilizable storage capacity of 76.52%) respectively. April 2020 was the month with the highest extreme dry conditions with SPI, rainfall, air temperature and water level values at -3.25, 20 mm, 21.2 ℃ and 450.95 m respectively (utilizable storage capacity of 93.41%).

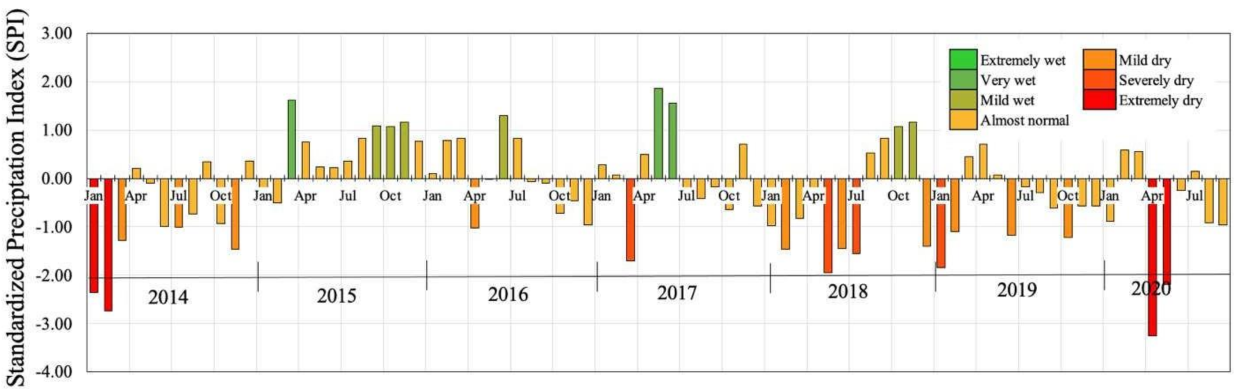

Figure 2. SPI time series from 2014 to 2020.

The return period of dry conditions, estimated following the approach by McKee et al. (1993), was calculated for the time series in this study (Table 2). The analysis revealed that the extreme droughts observed in 2014 and 2020 occurred once every 50 years. It also showed that the two extreme droughts of 2014 and 2020 happened rarely.

Table 2. Return period of drought events.

SPI	Category	Return period
0 to -0.99	Mild dryness	1 every 3 years
-1.00 to -1.49	Moderate dryness	1 every 10 years
-1.5 to - 1.99	Severe dryness	1 every 20 years
-2.00 or less	Extreme dryness	1 every 50 years

3.2. Precipitation, air temperature and water level

Precipitation, air temperature and water level time series are displayed in Figure 3a and b. Considering the values for January 2014, the maximum, minimum and average values of air temperature were 26.26, 24.03 and 25.21℃ respectively. The maximum, minimum, and average amount of rainfall were 355, 104 and 214.50 mm respectively. For the water level, the maximum, minimum and average values were 449.64, 447.24 and 448.22 m respectively. In April 2020, the maximum, minimum, and average of air temperature, rainfall and water level were 23.46, 21.21 and 22.42℃, 122, 20 and 65 mm, 451.09, 450.13, and 450.67 m respectively.

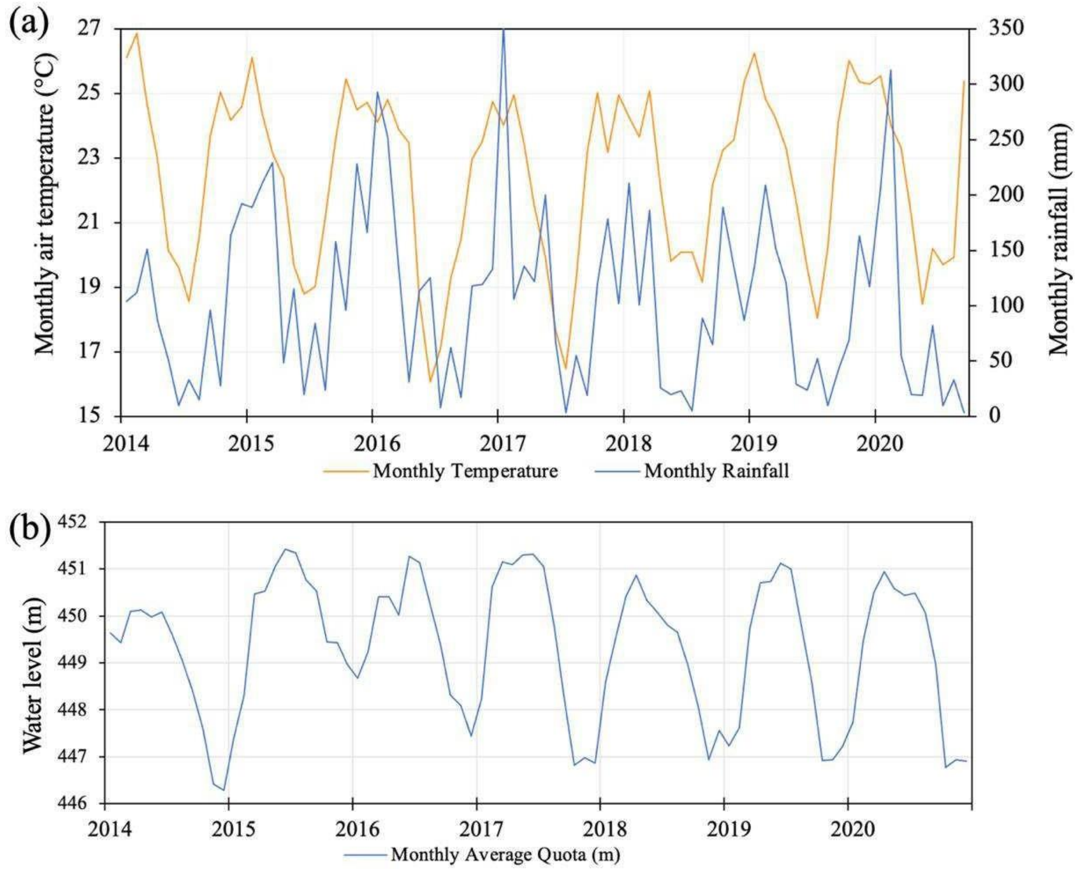

Figure 3. Monthly air temperature and rainfall (a) and monthly average water level (b).

3.3. Chlorophyll-a algorithm validation and application

The tuned algorithm (Equation 2) was validated with field data and the results showed an NRMSE of 18.92% (bias of -0.20 $mg.m^{-3}$). The error in estimating Chl-*a* from satellite images may be high because of the reduced absorption spectra (Marra et al., 2007). However, Alcântara et al. (2016) used the same dataset to evaluate the phytoplankton package effect on the Chl-*a* specific absorption coefficient (a^*_{phy}) and concluded that this effect was more pronounced for Chl-*a* concentrations > 200 mg m^{-3}. Therefore, the use of satellite-based estimations of Chl-*a* concentration was validated, and the algorithm was applied to 50 OLI/Landsat-8 images. Figure 4 shows a set of 16 selected processed images for the study site during this period. The regions where high values (red) were next to the dam and the Piracicaba River.

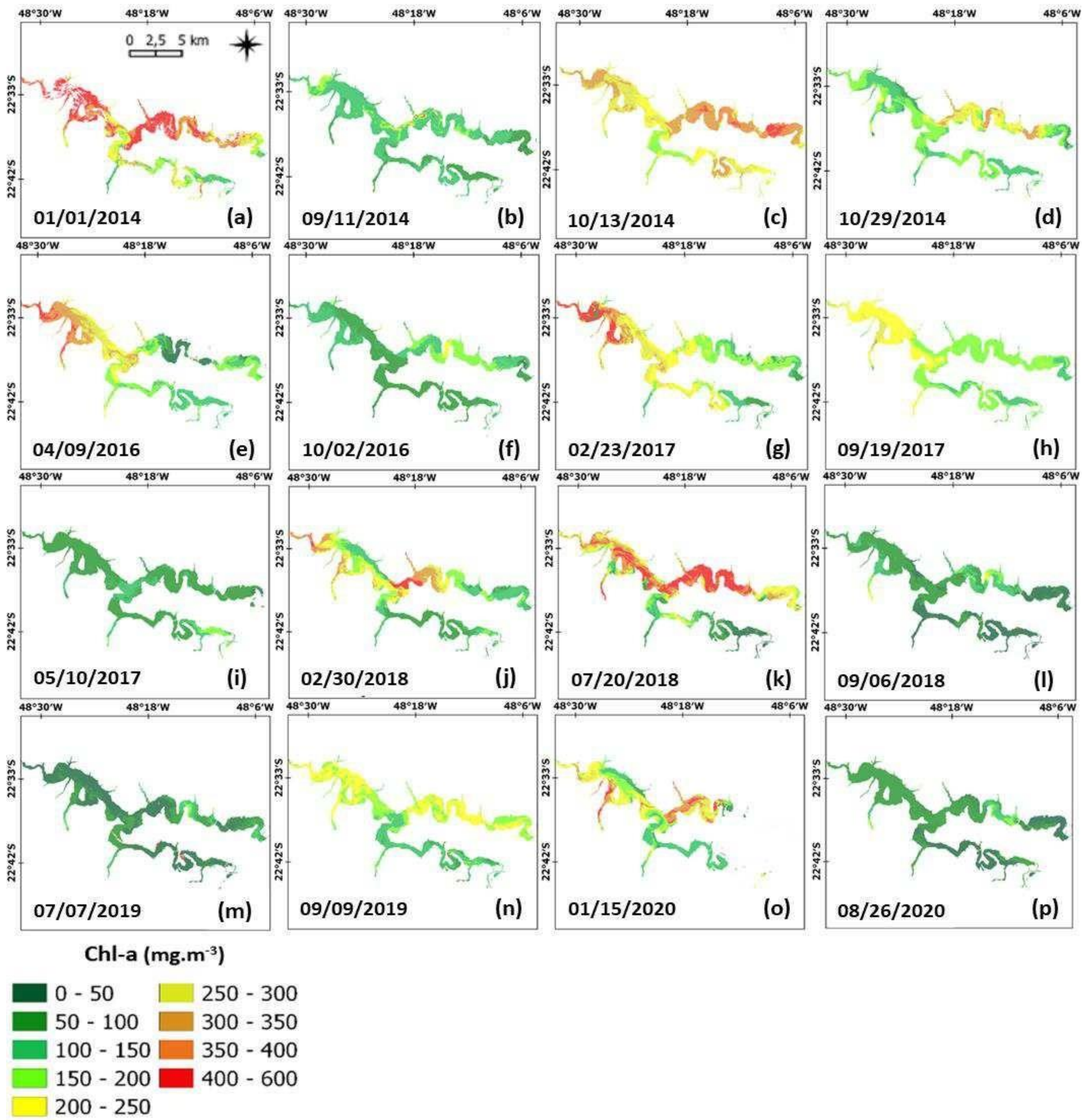

Figure 4. Selected Chl-*a* maps showing the spatial distribution within the BBHR between 2014 to 2020, estimated using the Slope tuned algorithm.

To better understand the variability in Chl-*a* from 2014 to 2020, we display a boxplot that used all 50 images (Figure 5). In summer, Chl-*a* concentrations tend to be high. The Chl-*a* concentration during the extreme drought in January 2014 ranged from 9 to 1068 mg m^{-3}, and in April 2020, the Chl-*a* concentration ranged from 3 to 902 mg m^{-3}. Since no cloud-free satellite images were available after January 2014, only Chl-

a data for September were analyzed (Chl-*a* ranged from 2 to 724 mg m^{-3}). However, after April 2020, the next available image was for July (Chl-*a* ranged from 3 to 755 mg m^{-3}). Notably, the three highest Chl-*a* concentrations were found in March 2017 (austral autumn) (Chl-*a* ranged from 2 to 1625 mg m^{-3}), August 2018 (austral winter) (Chl-*a* ranged from 3 to 1463 mg m^{-3}), and August 2020 (austral winter) (Chl-*a* ranged from 2 to 1267 mg m^{-3}). The SPI for March 2017, August 2018 and August 2020 were 0.50 (almost normal), 0.53 (almost normal) and -0.92 (almost normal) respectively. The air temperature and rainfall values were 21.5℃ (122 mm), 19.15℃ (89 mm) and 19.92℃ (33 mm) respectively. Lastly, the water level and useful volume were 451.14 m (95.73%), 449.65 m (78.81%) and 450.06 m (83.35%) respectively.

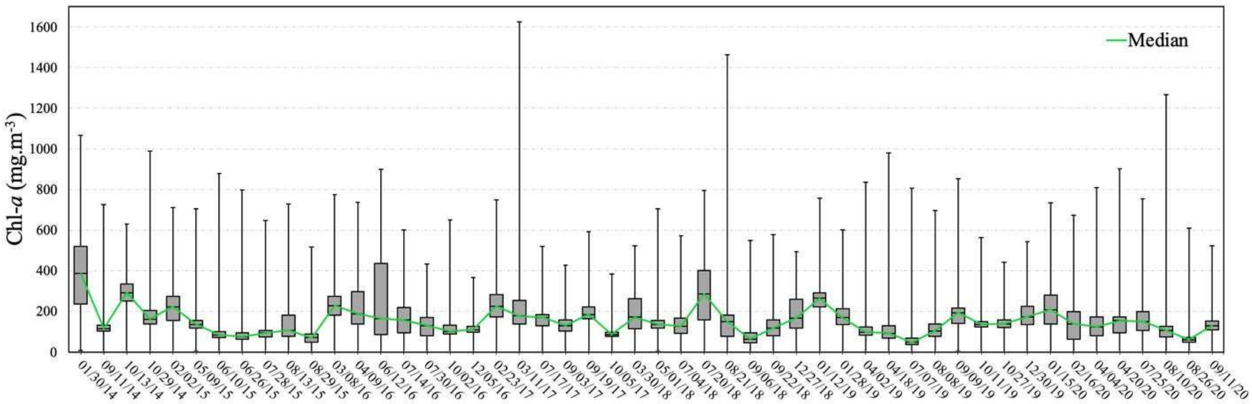

Figure 5. Boxplot showing the distribution of Chl-*a* concentration from 2014 to 2020.

3.4. Chl-a time series fitting distributions

The results of the fitting distributions applied to the Chl-*a* time series are presented in Table 3. The highest p-values from the Kolmogorov–Smirnov test were logistic, normal, and Weibull distributions. The logistic and normal distributions were statistically equal and very close to the Weibull fitting.

Table 3. Kolmogorov–Smirnov test results for fitted distributions to the Chl-*a* time series.

Distribution	*p*-value
Exponential	<0.0001
Fisher-Tippett	<0.0001
Gamma	0.861
Gumbel	<0.0001
Log-normal	0.632
Logistic	0.922
Normal	0.923
Student	<0.0001
Weibull	0.945

The Chl-a dataset was better represented by the Weibull distribution (Figure 6), with p-value (two-tailed) from the Kolmogorov–Smirnov test equal to 0.945 (alpha = 0.05) and D = 0.082.

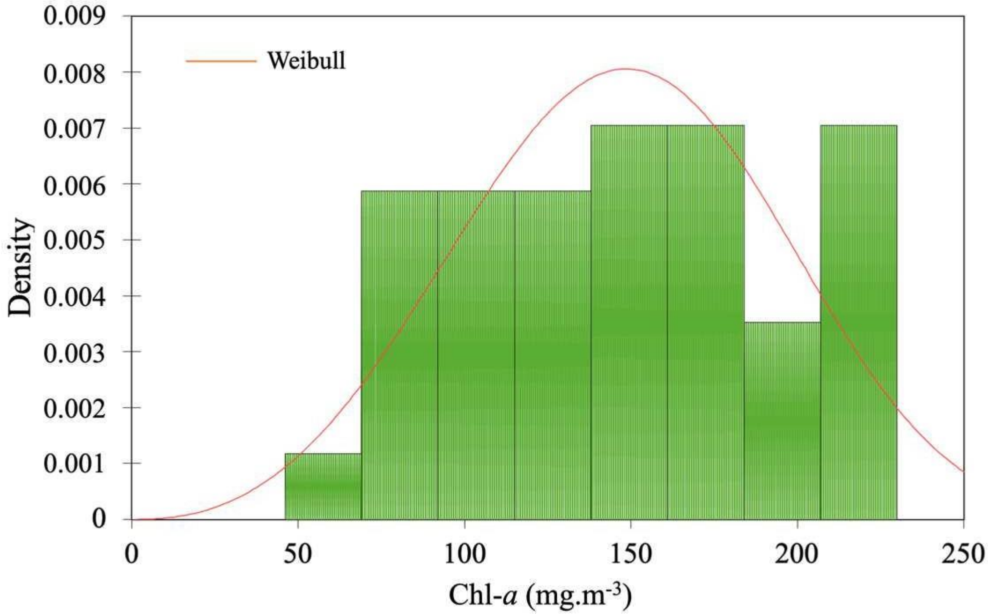

Figure 6. Chl-*a* time series fitted using a Weibull distribution.

The Weibull distribution showed that the main density for Chl-*a* concentrations ranged from 150 to 170 mg m^{-3} and 210 to 230 mg m^{-3}; and the lowest density ranged from 50 to 80 mg m^{-3}. High concentrations of Chl-*a* were uncommon after calculating the average Chl-*a* from the satellite images.

A DW test was applied to the Chl-*a* time series to verify the presence of autocorrelation. Autocorrelation refers to the degree of similarity between a given time series and lagged version over successive time intervals. The DW test showed that the residuals of the Chl-*a* time series were not autocorrelated because the p-value was greater than the significance level α= 0.05 (Table 4). Therefore, the Chl-*a* concentrations estimated by the satellite images were independent of each other.

Table 4. Durbin–Watson test results for Chl-*a* time series.

DW	1.635
p	0.155
p-value (one-tailed)	0.191
α	0.050

The results from the Augmented Dickey–Fuller test show that the computed p-value was lower than the significance level α= 0.05. Therefore, the null hypothesis should be rejected, which means that the Chl-*a* time series is stationary (Table 5). In a stationary process, the mean, variance, and autocorrelation structure do not change over time. From Figure 4, we can see variability in Chl-*a*; however, this cyclicity was not significant over time. This may occur because the satellite data have a short time resolution that prevents it from capturing the Chl-*a* bloom during our study period.

Table 5. Augmented Dickey–Fuller test results for Chl-*a* time series.

τ (Observed value)	-5.106
τ (Critical value)	-3.513
p-value (one-tailed)	0.001
α	0.05

The Mann–Kendall test shows that the computed *p*-value was greater than the significance level $\alpha = 0.05$; therefore, we cannot reject the null hypothesis—i.e., a trend was detected in the Chl-*a* time series. A trend is a pattern in data that shows the movement of a series to relatively higher or lower values over a long period of time. Sen's slope was -0.481 (Table 6), indicating a negative trend.

Table 6. Mann–Kendall and Sen's slope test results for Chl-*a* time series.

Kendall's τ	-0.056
S'	-17.000
Var(S')	1393.000
p-value (Two-tailed)	0.668
α	0.050

3.5. Trophic Status Index versus SPI

The TSI was calculated from the Chl-*a* derived from satellite images, and a boxplot of the TSI for each SPI class was plotted (Figure 7). For mildly wet conditions, only one median value of TSI was identified. However, an increase in TSI from almost normal to extremely dry conditions was evident. In general, mildly wet, mildly dry, severely dry, and extremely dry events resulted in TSI being classified as eutrophic while almost normal events meant that TSI was classified as hypereutrophic. The rule was that $54 < TSI \leq 74$ indicated eutrophic waters and $TSI > 74$ indicated hypereutrophic waters.

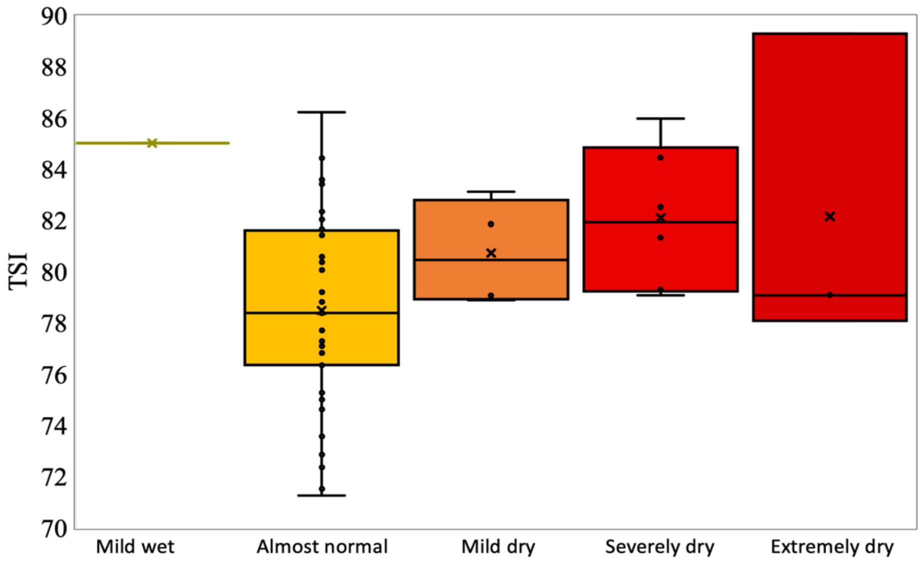

Figure 7. Boxplot of TSI based on the Chl-*a* estimated by satellite images by SPI class.

The almost normal events showed the highest variability in TSI from minimum to maximum. The TSI median was higher for severely dry events than for extremely dry ones; however, higher values of TSI were observed during extremely dry events.

3.6. Correlation between Chl-a and meteorological data

The time-window correlation coefficients between Chl-*a* and air temperature, rainfall, SPI, and water level are shown in Figure 8. This graph shows the correlation using windows of 6 × 6 months. In 2014, the correlations between Chl-*a* and air temperature, rainfall, SPI, and water level were 0.79, 0.26, -0.97 and -0.34 respectively. Chl-*a* had the highest (negative) correlation with the SPI in 2014. In 2020, the correlations were 0.54, 0.42, 0.04 and -0.59 respectively. Water level showed a positive correlation for those years that had mildly wet to almost normal events.

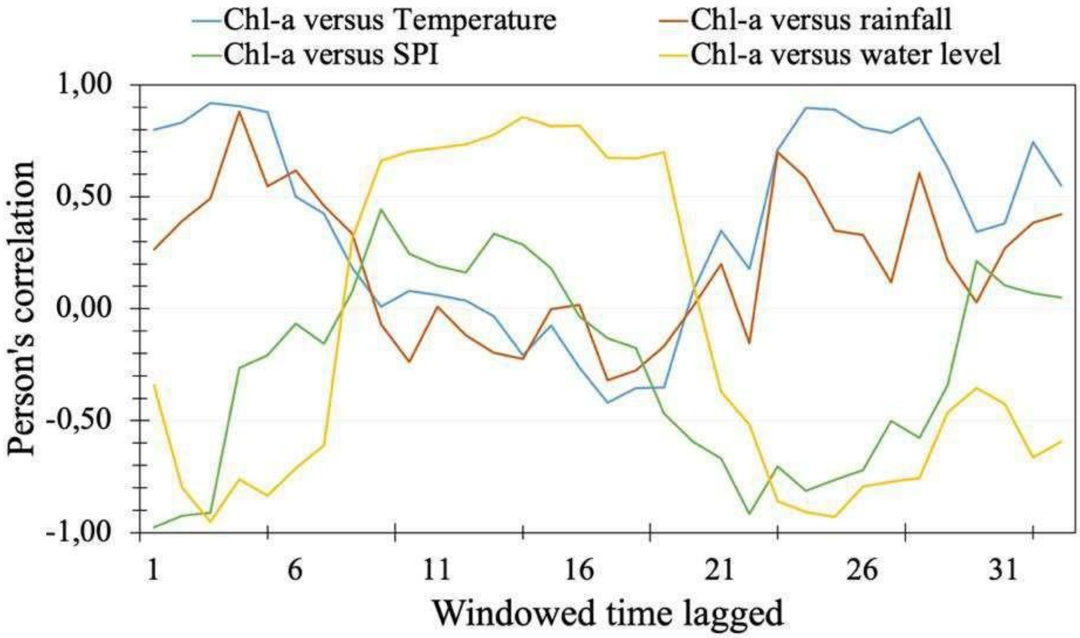

Figure 8. Windowed time lagged (6 × 6 months) Pearson's correlation between Chl-*a* concentration versus air temperature, rainfall, SPI, and water level.

4. Discussion

4.1 Use of Earth Observation for phytoplankton biomass monitoring

The use of remote sensing for monitoring water quality in inland waters has expanded over the last two decades (Ogashawara, 2021). Recently, several studies have explored the use of satellite imagery to create time-series of algal information, especially from sensors of the Landsat family, which is a long-term mission of Earth Observation data acquisition (Ho et al., 2019, Kuhn and Butman, 2021, Hou et al., 2022, Fang et al., 2022). However, based on the methodology used in these studies, only floating phytoplankton biomass was considered because none of these studies used aquatic atmospheric correction (suitable for aquatic environments, especially inland waters). Ho et al. (2019) and Fang et al. (2022) did not use atmospherically corrected data; therefore, the information retrieved by these studies did not consider the effects of the atmosphere or sun glint, sky glint, and adjacency. Hou et al. (2022) used a surface reflectance product but the product they used did not consider the effects of sun glint and adjacency of the surrounding land. In this study, we also used a surface reflectance product, which had been validated in previous studies (Bernardo et al., 2017, Silva et al., 2021). Although the product was validated for some images, we note that the time-series analysis can still be affected by sun glint and adjacency effects of the surrounding area of the BBHR.

While the use of Earth Observation for the estimation of Chl-*a* concentration was found to be accurate in some studies (Moses et al., 2009, Matthews, 2011, Mishra and Mishra, 2012), its use for monitoring nutrients is an underdeveloped process. Therefore, the use of Earth Observation for the estimation of nutrients is based on empirical relationships, and we could not establish a reliable time series of nutrient data to enhance our analysis. Nevertheless, the physicochemical properties and accelerated eutrophication of BBHR were likely caused by human interference (Matsumura-Tundisi and Tundisi, 2005; Buzelli and Cunha-Santino, 2013; Rietzler et al., 2018). Limnological variables were also compromised by wastewater and agricultural activities (Silva et al., 2022).

4.2 Phytoplankton biomass dynamics

Climate variability has altered rainfall regimes, affecting reservoir storage, stream flow, soil moisture, and water availability in southeastern Brazil. The Tietê River where the BBRH was located, had its water storage capacity reduced to approximately 3% owing to the most severe drought in 2014 (Coelho et al., 2016, Nobre et al., 2016). During this period, the water flux at the dam was controlled and the water retention time increased, making the reservoir a suitable place for phytoplankton growth.

Higher Chl-*a* concentrations were associated with higher light and nutrient availability during the austral summer (Figure 4) and this was consistent with the in-situ observations by Odebrecht et al. (2015). The study area experienced an extremely dry event in January and February 2014 (Figure 5) owing to a precipitation deficit (Coelho et al., 2015) and this low precipitation rate, combined with the high retention time, led to an increase in the Chl-*a* concentration in January. This phenomenon was also observed by Londe et al. (2016), who concluded that an increase in water residence time made the reservoir surface full of phytoplankton bloom.

Compared to the drought in 2020, the extreme drought in 2014 was more positively correlated with air temperature; however, a positive pattern was also observed in 2020. This indicates that an increase in air temperature has increased phytoplankton biomass, whereas a decrease in the SPI will increase phytoplankton biomass. Increasing air temperature also affects primary productivity, solubility, nutrient biogeochemical cycling, reaction rates, soil moisture, and other factors related to water quality (Coffey et al., 2018)

BBHR was classified as a eutrophic-hypertrophic waterbody (Figure 7), which confirms that eutrophication in the reservoir was a result of several processes, such as land-use land cover changes in the watershed, diffuse and specific pollution, and hydropower operation (high water retention time). Salk et al. (2022) used an experiment on eutrophication in lakes and showed that increases in water temperature associated with climate change can lead to earlier and larger phytoplankton blooms. Therefore, the use of meteorological and climatological data should always be considered in the assessment and modelling of water quality and this includes the use of the maximum air temperature.

The hydrological cycle has been modified by climate change and increasing eutrophication potential creates favorable conditions for cyanobacterial growth (Paerl and Paul, 2012). Cyanobacterial harmful algal blooms (cHABs) are a serious public health issue worldwide because of their ability to form dense biomass-producing toxins. cHABs toxins can cause gastrointestinal distress, dermatitis, liver failure, and death in domestic and livestock animals (Stumpf et al., 2016, Alcântara et al., 2021). This is an important finding for BBHR because the São Paulo State Environmental Agency (CETESB) annual reports (CETESB 2011–2015) showed that BBHR was mostly dominated by cyanobacteria, including potential cHAB toxin producers. The 2014 and 2020 droughts started as meteorological events that led to hydrological droughts. A meteorological drought is associated with periods of low rainfall, high temperatures and high evaporation rates. Meanwhile, water shortages are caused by hydrological droughts and such droughts can increase water retention time. In addition, the increasing of air temperature due to climate change can influence the heating and cooling of aquatic systems, altering water column mixing and stratification patterns and increasing the potential of algal blooms (Alcântara et al., 2010). The phytoplankton species richness in reservoirs such as BBHR is influenced by water column mixing and retention time (Matsumura-Tundisi and Tundisi, 2005) and the predominance of determined species is associated with water column stability (Tundisi et al., 2010).

Alcântara et al. (2010) studied the pattern of water column mixing and stratification in the Itumbiara Reservoir, located between Minas Gerais and Goiás states in Brazil. From January (austral summer) to May (austral autumn) and from August (austral winter) to December (austral summer), the water column stratifies. Conversely, from May to August, the water column mixes. Cyanobacterial blooms generally occur when the retention time is longer, whereas diatoms and Chlorophyta have shorter retention times (Perry et al., 1990).

BBHR is polymitic with a short period of column stability; the planktonic community structure and succession of species rapidly change due to cold fronts and retention time. During water column stability, blooms of Microcystis sp. are common. Human activities in watersheds, such as untreated wastewater, high suspended material, and fertilizers from agriculture, have a considerable impact on primary productivity (Tundisi, Matsumura-Tundisi and Abe, 2008). This highlights the importance of long-term monitoring programs for algal blooms and using it to evaluate the influence of extreme climatic events such as droughts.

5. Conclusion

The slope index used to derive the Chl-*a* concentration was suitable for application to OLI/Landsat-8 images, with an NRMSE of 18.92% and bias of -0.20 mg. m^{-3}. High concentrations were observed during the summer in BBHR, especially in January and February. The same period that experienced extreme drought events in 2014 was also confirmed using the SPI time series analysis. The Chl-*a* concentration was positively correlated (r=0.79) with air temperature and negatively correlated with SPI (r=-0.97) in 2014. These results indicate an increase in algal biomass due to high air temperatures and low SPI. In 2020, another extreme drought event was observed, where the Chl-*a* concentration was positively correlated with air temperature (0.54) and negatively correlated (-0.59) with water level. Our results suggest an unexpected dynamic for the occurrence of phytoplankton blooms, which are usually associated with the transport of nutrients from agricultural land to aquatic systems via rainfall. Therefore, our findings show the need for further investigation, especially for the identification of phytoplankton species, to improve water quality monitoring, especially with climatic variability. Lastly, this assessment was supported by the recurrence probability of drought events, which meant that such similar events may occur once every 50 years.

Funding

This work was supported by the São Paulo Research Foundation (FAPESP) under Grant 2019/00259-0.

References

Abe, D.S., Magsumura-Tundisi, T., Rocha, O., Tundisi, J.G., 2003. Denitrification and bacterial community structure in the cascade of six reservoirs on a tropical river in Brazil. Hydrobiologia, 504, 67-76. https://doi.org/10.1023/B:HYDR.0000008509.47900.fc

Adrian, R., *et al* 2009. Lakes as sentinels of climate change. Limnology and Oceanography. 54, 2283-2297. https://doi.org/10.4319/lo.2009.54.6_part_2.2283

Alcântara, E.H., Stech, J.L., Lorenzzetti, J.A., Bonnet, M-P., Casamitjana, X., Assireu, A.T., Novo, E.M.L.M 2010. Remote sensing of water surface temperature and heat flux over a tropical hydroelectric reservoir. Remote Sensing of Environment 114, 2651-2665. https://doi.org/10.1016/j.rse.2010.06.002

Alcântara, E., Watanabe, F., Rodrigues, T., Bernardo, N 2016. An investigation into the phytoplakton package effect on the clorophyll-a specific absorption coefficient in Barra Bonita reservoir, Brazil. Remote Sensing Letters. 7, 761-770. https://doi.org/10.1080/2150704X.2016.1185189

Arlot, S., Celisse, A 2010. A survey of cross-validation procedures for model selection. Stat. Surv., 4, 40-79. https://doi.org/10.1214/09-SS054

Barbosa, F.A.R. *et al*. 1999. The cascading reservoir continuum concept (CRCC) and its application to the river Tietê-basin, São Paulo State, Brazil. In *Theoretical reservoir ecology and its application*; Tundisi, J.G., Straškraba, M. (Eds.). International Institute of Ecology: São Carlos, Brazil, pp. 425-437.

Barsi, J.A., Lee, K., Kvaran, G., Markham, B.L., Pedelty, J.A. 2014. The Spectral Response of the Landsat-8 Operational Land Imager. Remote Sensing 6, 10232-10251. https://doi.org/10.3390/rs61010232

Behrenfeld, M.J., Boss, E.S. 2014. Resurrecting the ecological underpinnings of ocean plankton blooms. Ann Rev Mar Sci 6:167–194. https://doi.org/10.1146/annurevmarine-052913-021325

Berger, SA., Diehl, S, Stibor, H, Trommer, G, Ruhenstroth, M. 2010. Water temperature and stratification depth independently shift cardinal events during plankton spring succession. Glob. Change Biol. 16: 1954-1965. https://doi.org/10.1111/j.1365-2486.2009.02134.x

Bernardo, N., Alcântara, E., Watanabe, F., Rodrigues, T., Carmo, A., Gomes, A., Andrade, C. 2018. Glint Removal Assessment to Estimate the Remote Sensing Reflectance in Inland Waters with Widely Differing Optical Properties. Remote Sens. 10, 1655. https://doi.org/10.3390/rs10101655

Buzelli, G., M., Cunha-Santino, M., B. 2013. Análise e diagnóstico da qualidade da água e estado trófico do reservatório de Barra Bonita. SP. Rev Ambiente Amp Água 8, 186–205. https://doi.org/10.4136/ambi-agua.930

Carlson, R., E. 1977. A trophic state index for lakes. Limnol Oceanogr 22:361–369. https://doi.org/10.4319/lo.1977.22.2.0361

CETESB. 2011–2015. Relatórios Anuais de Águas Interiores, Companhia Ambiental do Estado de São Paulo [Annual reports on inland waters, São Paulo State Environmental Company]. http://cetesb.sp.gov.br/aguasinteriores/publicacoes-e-relatorios

Coelho, C. A. S., Oliveira, C.P., Ambrizzi, T. *et al.* 2016. The 2014 southeast Brazil austral summer drought: regional scale mechanisms and teleconnections. Clim Dyn 46:3737–3752. https://doi.org/10.1007/s00382-015-2800-1

Coffey, R., Paul, M., Stamp, J., Hamilton, A., Johnson, T. 2018. A review of water quality responses to air temperature and precipitation changes 2: nutrients, algal blooms, sediment, pathogens. Journal of the American Water Resources Association. 55, 844-868. https://doi.org/10.1111/1752-1688.12711

Correa, D., B., Alcântara, E., Libonati, R., Massi, K., G., Park, E. 2022. Increased burned area in Pantanal over the past two decades. Science of The Total Environment. 835, 155386. https://doi.org/10.1016/j.scitotenv.2022.155386

Cunha, A., P., M., A. *et al* 2019. Extreme drought events over Brazil from 2011 to 2019. Atmosphere. 10, 642. https://doi.org/10.3390/atmos10110642

Elliot, J., A. 2012. Predicting the impact of changing nutrient load and temperature on the phytoplankton of England's largest lake, Windermere. Freshw. Biol., 57, 400-413. https://doi.org/10.1111/j.1365-2427.2011.02717.x

Elliot, J., A., Jones, I., D., Thackeray, S., J. 2006. Testing the sensitivity of phytoplankton communities to changes in water temperature and nutrient load, in a temperate lake. Hydrobiologia 559, 401-411. https://doi.org/10.1007/s10750-005-1233-y

Fang, C., Song, K., Paerl, H., W,, Jacinthe, P., A., Wen, Z., Liu, G., Tao, H., Xu, X., Kutser, T., Wang, Z., Duan, H., Shi, K., Shang, Y., Lyu, L., Li, S., Yang, Q., Lyu, D., Mao, D., Zhang, B., Cheng, S., Lyu, Y. 2022. Global divergent trends of algal blooms detected by satellite during 1982-2018. Global Change Biology 28, 327-2340. https://doi.org/10.1111/gcb.16077

Getirana, A. 2016. Extreme water deficit in Brazil detected from space. J Hydrometeorol 17, 591-599. https://doi.org/10.1175/JHM-D-15-0096.1

Getirana, A., Libonati, R., Cataldi, M. 2021. Brazil is in water crisis - it needs a drought plan. Nature, 600, 218-220. *https://doi.org/10.1038/d41586-021-03625-w*

Gittings, J. A., Raitsos, D. E., Krokos, G., Hoteit, I. 2018. Impacts of warming on phytoplankton abundance and phenology in a typical tropical marine ecosystem. Sci. Rep. 8, 2240. https://doi.org/10.1038/s41598-018-20560-5

Golterman H.L., Clymo, R.S., Ohnstad, M.A.M., 1978. Methods for Physical and Chemical Analysis of Freshwater. Blackwell Scientific Publications, Oxford. https://doi.org/10.1002/iroh.19800650113.

Gons, H.J. 1999. Optical teledetection of chlorophyll-a in turbid inland waters. Environmental Science and Technology 33, 1127-1132. https://doi.org/10.1021/es9809657

Haan, C.T., 1977. Statistical methods in hydrology. The Iowa University Press, Iowa, U.S.A.

Hallegraeff, G.M., Anderson, D.M., Belin, C. *et al.* 2021. Perceived global increase in algal blooms is attributable to intensified monitoring and emerging bloom impacts. Commun Earth Environ 2, 117. https://doi.org/10.1038/s43247-021- 00178-8

Ho, J.C., Michalak, A.M., Pahlevan, N. 2019. Widespread global increase in intense lake phytoplankton blooms since the 1980s. *Nature* 574, 667–670. https://doi.org/10.1038/s41586-019-1648-7

Hou, X., Feng, L., Dai, Y. *et al.* 2022. Global mapping reveals increase in lacustrine algal blooms over the past decade. Nature Geosciences 15, 130–134. https://doi.org/10.1038/s41561-021-00887-x

Kuhn, C., Burman, D. 2021. Declining greenness in Arctic-boreal lakes. Proceedings of the National Academy of Sciences. 118, e2021219118. https://doi.org/10.1073/pnas.2021219118

Lee, Z., Ahn, Y., Mobley, C., Arnone, R. 2010. Removal of surface-reflected light for the measurements of remote-sensing reflectance from an above-surface platform. Opt. Exp, 18, 26313–26324. https://doi.org/10.1364/OE.18.026313

Londe, L.R., Novo, E.M.L.M., Barbosa, C., Araujo, C.A.S. 2016. Water residence time affecting phytoplankton blooms: study case in Ibitinga Reservoir (São Paulo, Brazil) using Landsat/TM images. Brazilian Journal of Biology 76, 664-672. https://doi.org/10.1590/1519-6984.23814

Maberly, S.C., Hurley, M.A., Butterwick, C., Corry, J.E., Heaney, S.I., Irish, A.E., *et al.*

1994. The rise and fall of Asterionella formosa in the South Basin of Windermere: Analysis of a 45-year series of data. Freshw. Biol. 31, 19-34. https://doi.org/10.1111/j.1365-2427.1994.tb00835.x

Marengo, J.A., Cunha, A.P., Cuartas, L.A., Deusdará, L.K.R., Broedel, E., Seluchi, M.E., Michelin, C.M., Baião, C.F., Chuchón, A. E,, Almeida. E.K., Kazmierczak, M.L., Mateus, N.P.A., Silva, R.C., Bender, F. 2021. Extreme Drought in the Brazilian Pantanal in 2019–2020: Characterization, Causes, and Impacts. Front. Water 3:639204. https://doi.org/ 10.3389/frwa.2021.639204

Marra, J., Trees, C.C., O'Reilly, J.E. 2007. Phytoplankton Pigment Absorption: A Strong Predictor of Primary Productivity in the Surface Ocean. Deep Sea Research Part I: Oceanographic Research Papers 54, 155-163. https://doi.org/10.1016/j.dsr.2006.12.001

Matsumura-Tundisi, T., Tundisi, J.G. 2005. Plankton richness in a eutrophic reservoir (Barra Bonita reservoir, SP, Brazil). Hydrobiologia 542, 367–378. https://doi.org/10.1007/s10750-004-9461-0

Matthews, M.W. 2011. A current review of empirical procedures of remote sensing in Inland and near-coastal transitional waters. Int. J. Remote Sens. 32, 6855-6899. https://doi.org/10.1080/01431161.2010.512947

McKee, T.B., Doesken, N.J., Kleist, J. 1993. The relationship of drought frequency and duration to time scales. In: Eight Conference on Applied Climatology, pp 179-184.

Mishra, R.D., Mishra, S. 2010. Plume and bloom: effect of the Mississippi River diversion on the water quality of Lake Pontchartrain. Geocarto International. 25, 555-568. https://doi.org/10.1080/10106041003763394

Mishra, S., Mishra, D.R. 2012. Normalized difference chlorophyll index: A novel model for remote estimation of chlorophyll-a concentration in turbid productive waters. Remote Sens. Environ., 117, 394-406. https://doi.org/10.1016/j.rse.2011.10.016

Mobley, C.D. 1999. Estimation of the remote-sensing reflectance from above-surface measurements. Appl. Opt. 38, 7442-7455. https://doi.org/10.1364/AO.38.007442.

Moses, W.J., Gitelson, AA., Berdnikov, S, Povazhnyy, V. 2009. Estimation of chlorophyll-a concentration in case II waters using MODIS and MERIS data - Successes and challenges. Environ. Res. Lett. 4, 04500. https://doi.org/10.1088/1748-9326/4/4/045005

Nobre, C., Marengo, J., Seluchi, M., Cuartas, L., Alves, L. 2016. Some Characteristics and Impacts of the Drought and Water Crisis in Southeastern Brazil during 2014 and 2015. Journal of Water Resource and Protection, 8, 252-262. doi: 10.4236/jwarp.2016.82022.

Odebrecht, C., Abreu, P.C., Carstensen, J. 2015. Retention time generates short-term phytoplankton blooms in a shallow microtidal subtropical estuary. Estuarine, Coastal and Shelf Science, 162, 35-44. https://doi.org/10.1016/j.ecss.2015.03.004

Ogashawara, I. 2021. Bibliometric Analysis of Remote Sensing of Inland Waters Publications from 1985 to 2020. *Geographies*, 1, 346-361. https://doi.org/10.3390/geographies1030019

Paerl, H.W., Hall, N.S., Peierls, B.L., Rossignol, K.L. 2014. Evolving paradigms and challenges in estuarine and coastal eutrophication dynamics in a culturally and climatically stressed world. Estuar. Coasts, 37, 243-258. https://doi.org/10.1007/s12237-014-9773-x

Ridder, N. N. *et al.* 2020. Global hotspots for the occurrence of compound events. Nat. Commun.11, 1–10. https://doi.org/10.1038/s41467-020-19639-3

Rietzler, A.C., Botta, C.R., Ribeiro, M.M., Rocha, O., Fonseca, A.L. 2018. Accelerated eutrophication and toxicity in tropical reservoir water and sediments: an ecotoxicological approach. Environ Sci Pollut Res 25, 13292–13311. https://doi.org/10.1007/s11356-016-7719-5

Rosenzweig, C. 2007. Assessment of observed changes and responses in natural and managed systems. In: Parry ML, Canziani OF, Palutikof JP, van der Linden PJ, Hanson CE, others, editors. *Climate change 2007—impacts, adaptation and vulnerability. Contribution of Working Group II to the Fourth.*

Salk, K.R., Venkiteswaran, J.J., Couture, R-M., Higgins, S.N., Paterson, M.J., Schiff, S.L. 2022. Warming combined with experimental eutrophication intensifies lake phytoplankton blooms. Limnology and Oceanography, 67, 147-158. https://doi.org/10.1002/lno.11982

Smayda, T.J. 1997. What is a bloom? A commentary. Limnol. Oceanogr. 42, 1132–1136.

https://doi.org/10.4319/lo.1997.42.5_part_2.1132

Silva, F.L., Fushita, Â.T., da Cunha-Santino, M.B. *et al*. 2022. Adopting basic quality tools and landscape analysis for applied limnology: an approach for freshwater reservoir management. Sustain. Water Resources Management 8, 65. https://doi.org/10.1007/s40899-022-00655-8

Silva, L., Alcântara, E., Park, E., Bernardo, N., Watanabe, F. 2021. A single semi-analytical algorithm to retrieve chlorophyll-a concentration in oligo-to-hypereutrophic waters of a tropical reservoir cascade. Ecological Indicators 120, 106913. https://doi.org/10.1016/j.ecolind.2020.106913

Smith, W.S., Espíndola, E.L.G., Rocha, O. 2014. Environmental gradient in reservoirs of the medium and low Tietê river: limnological differences through the habitat sequence. Acta Limnologica Brasiliensia, 26, 73-88. https://doi.org/10.1590/S2179-975X2014000100009

Toledo, A.P. 1990. Preliminary report on the studies to obtain an index for the evaluation of trophic status of warm tropical regions reservoirs. CETESB (Environmental Sanitation Technology Company), São Paulo.

Tundisi, J.G., Matsumura-Tundisi, T., Pereira, K.C., Luzia, A.P., Passerini, M.D., Chiba, W.A.C., Morais, M.A., Sebastien, N.Y. 2010. Cold fronts and reservoir limnology: an integrated approach towards the ecological dynamics of freshwater ecosystems. Braz J Biol 70, 815–824. https://doi.org/10.1590/S1519-69842010000400012

Tundisi, J.G., Matsumura-Tundisi, T., Abe, D.S. 2008. The ecological dynamics of Barra Bonita (Tietê River, SP, Brazil) reservoir: implications for its biodiversity. Brazilian Journal of Biology. 68, 1079-1098. https://doi.org/10.1590/S1519-69842008000500015

Watanabe, F.S.Y., Alcântara, E., Rodrigues, T.W.P., Imai, N.N., Barbosa, C.C.F., Rotta, L.H.S. 2015. Estimation of chlorophyll-a concentration and the trophic state of the Barra Bonita hydroelectric reservoir using OLI/Landsat-8 images. International Journal of Environment Research and Public Health, 12, 10391-10417. https://doi.org/10.3390/ijerph120910391

Watanabe, F., Rodrigues, T., Bernardo, N. *et al.* 2016. Drought can cause phytoplankton growth intensification in Barra Bonita reservoir. Model. Earth Syst. Environ. 2, 134. https://doi.org/10.1007/s40808-016-0193-8

Watanabe, F., Alcântara, E., Rodrigues, T., Rotta, L., Bernardo, N., Imai, N. 2018. Remote sensing of the chlorophyll-*a* based on OLI/Landsat-8 and MSI/Sentinl-2A (Barra Bonita reservoir, Brazil). Annals of the Brazilian Academy of Sciences. 90:1987-2000. https://doi.org/10.1590/0001-3765201720170125

Wilkinson, G.M., Walter, J.A., Buelo, C.D., Pace, M.L. 2022. No evidence of widespread algal bloom intensification in hundreds of lakes. Front Ecol Environm 20, 16-21. https://doi.org/10.1002/fee.2421

Williamson, C.E., Saros, J.E., Schindler, D.W. 2009. Sentinels of change. *Science.* 2009323, 887–889. https://doi.org/10.1126/science.116944

3 CONSIDERAÇÕES GERAIS

O aumento da degradação ambiental no último século causou significativo aumento na severidade e distribuição geográfica dos episódios de HABs (*harmful algal bloom*), tanto em lagos pequenos quanto grandes, em reservatórios e rios, e em outras superfícies aquáticas ao redor do globo. As variações observadas são referidas à fenologia do fitoplâncton, que é a característica de eventos naturalmente recorrentes como os ciclos sazonais. A abundância de fitoplâncton e sua fenologia podem ser definidas como um indicador ecológico e estudos têm comprovado que as mudanças climáticas atuam sobre a variabilidade natural do fitoplâncton (PLATT *et al.*, 2003; KOELLER *et al.*, 2009; GITTINGS *et al.*, 2018).

As mudanças climáticas locais, associadas às mudanças globais, também podem favorecer a proliferação das cianobactérias como os eventos mais longos e intensos de precipitação, que proporcionam o aumento do carreamento de nutrientes provenientes das bacias hidrográficas, tornando o corpo d'água um ambiente com potencial para as HABs, principalmente se estes episódios de chuvas foram seguidos por períodos de seca, o que tem sido cada vez mais observado desde meados dos anos 1990 (PAERL, HULSMAN, 2009; HALLEGRAEFF *et al.*, 2010).

Um cenário criado a partir de modelos de predição (IPCC RPC8.5) de floração de algas em águas oceânicas de altas, médias e baixas latitudes, considerando os primeiros 20 anos (2006- 2025) e os últimos 20 anos (2080-2099), previu como o tempo de floração do fitoplâncton se alteraria em resposta às mudanças climáticas projetadas para o século 21. A floração nos subtrópicos, no hemisfério norte, tenderá a se iniciar mais tarde (trocando seu início na primavera pelo início no outono). Em contrapartida, nos trópicos e no Oceano Antártico, a floração tenderá a ter seu início adiantado. Estes padrões observados são condizentes com a redução da amplitude sazonal da camada limnológica, que reduz a disponibilidade de nutrientes, fazendo com que as condições de floração nos subtrópicos do hemisfério norte se aproximem daquelas observadas nos trópicos.

Estima-se que as mudanças no tempo de floração ao redor do globo serão de ± 20 dias até o final deste século (HENSON *et al.*, 2017). Record *et al.* (2019) expuseram que com o aquecimento do clima, o verão torna-se mais longo, e deverá anteceder os episódios de floração na primavera no Golfo do Maine. Apesar de ser um fenômeno mundial, a maioria dos estudos publicados relacionando as toxinas das cianobactérias e HAB referem-se às zonas temperadas. Casos de cianobactérias já foram relatados no Brasil, Tailândia, Austrália, porém, o detalhamento desses casos pode enriquecer a discussão sobre a especificidade das regiões tropicais neste tipo de evento.

Os estudos de monitoramento da fenologia do fitoplâncton, a partir da utilização de dados de satélite, além do seu baixo custo, permitem o acesso remoto às informações da superfície terrestre de épocas passadas, considerando a necessidade de longos períodos (> 30 anos) de análise, como indica a Organização Mundial de Meteorologia (WMO), na identificação das mudanças impulsionadas pelo clima.

A clorofila-*a*, por estar presente em todas as espécies de fitoplâncton, é a medida mais próxima na determinação da biomassa fitoplanctônica, e pode ser relacionada aos dados espaciais. Modelos para estimativa de clorofila-*a* via dados de sensores remotos aplicados em águas interiores revelam a eficácia dessa abordagem (TOMLINSON *et al.*, 2015; MAEDA *et al.*, 2019).

Os reservatórios brasileiros estão sujeitos aos efeitos das mudanças climáticas (TRANVIK *et al.*, 2009), além das interferências de atividades que favorecem a eutrofização, que propiciam os eventos de HABs. Por apresentarem grande complexidade física, química e biológica, os reservatórios são um desafio à gestão da qualidade da água. Dessa forma, a compreensão e o monitoramento sistêmico dos eventos de HABs são medidas de auxílio aos órgãos gestores de corpos hídricos, além de permitirem a prevenção de desastres naturais que causam desequilíbrios ecossistêmicos e prejuízos à saúde pública.

REFERÊNCIAS

CURTARELLI, M. P.; ALCÂNTARA, E. H.; RENNÓ, C. D.; STECH, J. L. Physical changes within a large tropical hydroelectric reservoir induced by wintertime cold front activity. **Hydrology and Earth System Science,** v. 18, n. 8, p. 3079-3093, 2014.

MATSUMURA-TUNDISI, T.; TUNDISI, J. G. Phytoplankton richness in a eutrophic reservoir: Barra Bonita reservoir, SP, Brazil. **Hydrobiologia,** v. 542, n. 1, p. 367-378, 2005.

PERRY, S. A.; PERRY, W. B.; SIMMONS JUNIOR, G. M. Bacterioplankton and phytoplankton populations in a rapidly-flushed eutrophic reservoir. **Internationale Revue der gesamten Hydrobiologie und Hydrographie,** v. 75, n. 1, p. 24-44, 1990.

WATANABE, F.; RODRIGUES, T.; BERNARDO, N.; ALCÂNTRA, E. H.; IMAI, N. Drought can cause phytoplankton growth intensification in Barra Bonita reservoir. **Modeling Earth Systems and Environment,** v. 2, n. 134, 2016.